MORPHOLOGY OF γ' PRECIPITATES AFTER SIMPLE AGING IN FIRST STAGE LOW PRESSURE TURBINE BLADE OF Ni-BASED SUPERALLOY AFTER SERVICED[1]

Nobuhiro Miura[2]
Yoshihiro Kondo[3]

Abstract

To estimate the distribution of the temperature and the stress, and the stress direction of the blade in service, the morphology of the γ' precipitates in the Ni-based superalloy serviced as the 1st LPT blade of the aircraft engine and this aged one was investigated. Microstructure observations by a FE-SEM were carried out on the forty portions of the both sides of the perpendicular and the orthogonal sections at the vicinity of the blade surface in the suction and pressure sides. Most of the γ' precipitates kept cuboidal in shape in serviced blade. A lot of the secondary γ' precipitates in the γ matrix were observed at the root part. On the contrary, at the leading edge of the tip part, there were no secondary γ' precipitates. After simple aging, the low complete rafted γ/γ' structures were appeared at the suction sides of 70mm part, while the other portions, coarsening of the γ' precipitates was observed. Consequently, the 1st LPT blade in service, at the leading edge of the tip part was exposed to the highest temperature condition. However, the stress is extremely low in all portions.

Keywords: Superalloy; 1st stage low pressure turbine blade; γ' precipitates.

[1] *Technical contribution to the 18th IFHTSE Congress - International Federation for Heat Treatment and Surface Engineering, 2010 July 26-30th, Rio de Janeiro, RJ, Brazil.*

[2] *Lecturar, National Defense Academy.*

[3] *Proffesor, National Defense Academy.*

1 INTRODUCTION

As the material for turbine blade in aircraft engine, Ni-based superalloys have been employed because of their excellent in high temperature strengths and ductility.[1-6] It was well known that the cuboidal γ' precipitates of single crystal Ni-based superalloys with the stress axis of the [001] orientation turn their shapes into the plate like ones perpendicular to the stress axis during high temperature creep deformation.[7-11] It was impossible to measure the temperature and the stress of the blades in service, because the blades rotate with high speed at high temperature. Therefore, attention has focused on the evaluation method of the serviced condition of the blade based on the morphology of the γ' precipitates.[4-5,12] In our previous work, to estimate the temperature and the stress distribution of the blade in service, the morphology of the γ' precipitates of a single crystal Ni-based superalloy serviced as the first stage high pressure turbine (1st HPT) blade of a jet engine was examined. And it was possible to estimate the blade in service environment based on the morphology of the γ' precipitates qualitatively.[4]

By the way, the polycrystalline Ni-based superalloys have been used for 1st stage low pressure turbine (1st LPT) blade of a jet engine, because the gas temperature of 1st LPT was relatively low in comparison with that of HPT. However, in recent years, with a superior performance and a request of the carbon dioxide emissions reduction of the aircraft, the further high output and the high efficiency of the jet engine are demanded. The efficiency of the jet engine strongly depends on the Turbine Inlet Temperature (TIT) and becomes the high efficiency as a high temperature.[1,13] And so the TIT was steadily rising.[1] With an increase in the TIT, it was expected that the 1st LPT blade was exposed to the higher temperature. Moreover, the shape and size of the 1st LPT blade become complicated, namely large and long in the centrifugal direction compared with those of the 1st HPT one. In addition, the 1st LPT blade was non-cooled. Therefore, it was estimated that the temperature and the stress distribution of the 1st LPT blade were significantly different from those of the 1st HPT one. Based on the above conception, the microstructure observation was conducted on the 1st LPT serviced blade. The rafted γ/γ' structures were not observed, and most of the γ' precipitates kept cuboidal in shape. This microstructure evidence showed that the estimation of the stress distribution was difficult though the temperature was presumed to be low.[14]

In our previous work, the cuboidal γ' precipitates of the as-heat treated single crystal Ni-based superalloy, CMSX-4, connected to three <100> directions and coarsened with simple aging at the high temperature. On the contrary, by employing the aging without stress of CMSX-4 after the interrupted creep test at the stages when the γ' precipitates are still cuboidal, the γ/γ' structure changed to rafted one perpendicular to the creep interrupted stress axis.[15] Based on these experimental results, the formation of rafted γ/γ' structures corresponding to the stress history was expected by subjecting to the simple aging for serviced blade.

In this study, the morphological change in the γ' precipitates of the Ni-based superalloy serviced as the 1st LPT blade of the jet engine and the aged one was investigated to estimate the detail of the temperature and the stress distribution, and the stress directions in service.

2 EXPERIMENTAL PROCEDURE

A polycrystalline Ni-based superalloy was prepared in the form of the non-cooled turbine blade by precision casting. After employing the defined solution treatment and the aging, aluminized coating was done on the surface of the part of the airfoil. The blade was serviced as the 1st LPT blade of the jet engine on the military aircraft. The blade was cut into four parts of perpendicular to longitudinal direction at 10, 40, 70 and 90mm from the tip part by electron discharge machine. These parts were designated as the tip, 40mm, 70mm and root parts. Each part was cut into six portions parallel to the longitudinal direction from the leading edge to the trailing one at the interval of 7mm. Microstructure observations by a field emission electron microscope (FE-SEM) were carried out on the forty portions of the both sides of the perpendicular and the orthogonally sections at the vicinity of the interface between the coating layer and the matrix on the suction and pressure sides. These specimens were aged at 1273K, $3.6x10^6$s. SEM observations were also carried out on the aged specimens at the same portions before aging. Specimens for the SEM observation were prepared metallographically and electroetched with a supersaturated oxalic acid aqueous solution.

3 RESULTS

3.1 Appearance of 1st LPT Blade

The size of the airfoil of the 1st LPT blade is about 100mm maximum length, about 30mm maximum width. The change of color is observed at the leading edge of the pressure side and at the trailing edge of the suction side.

3.2 Morphology of γ' Precipitates in Different portion of Serviced Blade

3.2.1 Tip parts

The SEM micrographs at the pressure and suction sides of the tip part are shown in Fig.1. The dotted line on the photos are intersection lines of the orthogonal two planes, the upper side is perpendicular section on the boundary of this line, and the lower side is the orthogonally section. The right side of photos of the pressure side and the left side of photos of the suction side are parallel to the outside surface of the blade.

The cuboidal γ' precipitates becomes rounded in all portions. At the suction side, at the portion with the distance of 23mm from the leading edge, that is, 23mm portion, the fine secondary γ' precipitates are slightly observed in the γ matrix. The denuded zone of the secondary γ' precipitates are recognized at the matrix phase near the γ/γ' interfaces (Fig.1b). On the contrary, at the leading and trailing edge, there are few secondary γ' precipitates (Fig.1a and c). At the pressure side, the secondary γ' precipitates are only observed at the trailing edge, and the morphology and the distribution of ones are similar to the 23mm portion at the suction side (Fig.1e).

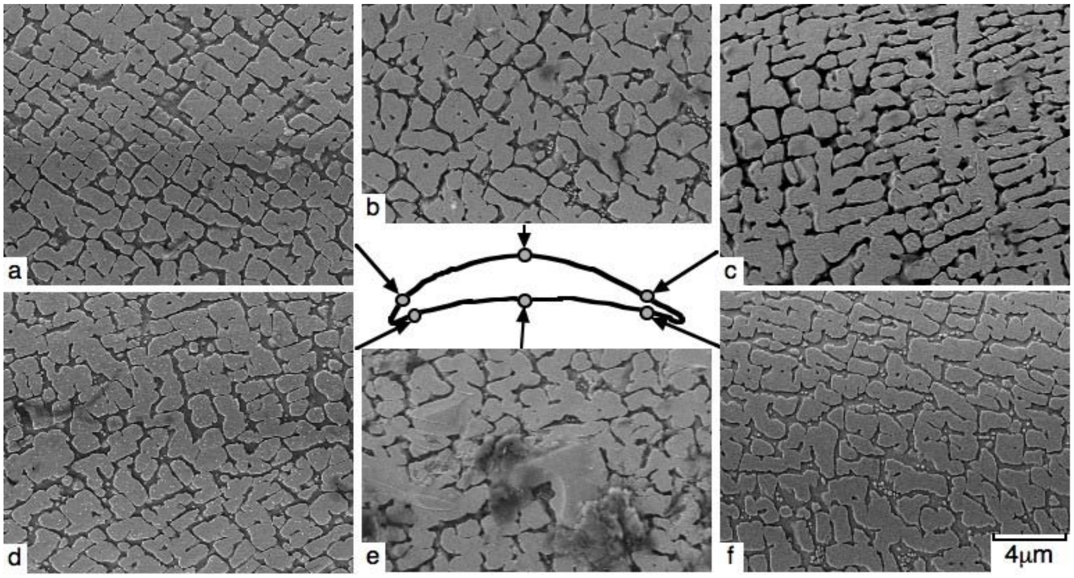

Figure 1. SEM micrographs of the suction and pressure sides of the tip part : the leading edge (a) and (d), 23mm portion (b) and (e) and the trailing edge (c) and (f), respectively.

3.2.2 40mm part

The SEM micrographs at the pressure and suction sides of the 40mm part are shown in Fig.2. At the suction side, most of the cuboidal γ' precipitates kept cuboidal in shape (Fig.2a-c). A lot of the fine secondary γ' precipitates are observed in the γ matrix at the 23mm portion and the trailing edge (Fig.2b,c). At the pressure side, the cuboidal γ' precipitates still remain as well as the suction side. No secondary γ' precipitates are observed at the leading edge (Fig.2d). However, the amount of the secondary γ' precipitates in the γ matrix increased toward the trailing edge(Fig.2d-f). And at the trailing edge, a large number of the secondary γ' precipitates are observed at the vicinity of the γ/γ' interfaces (Fig.2f).

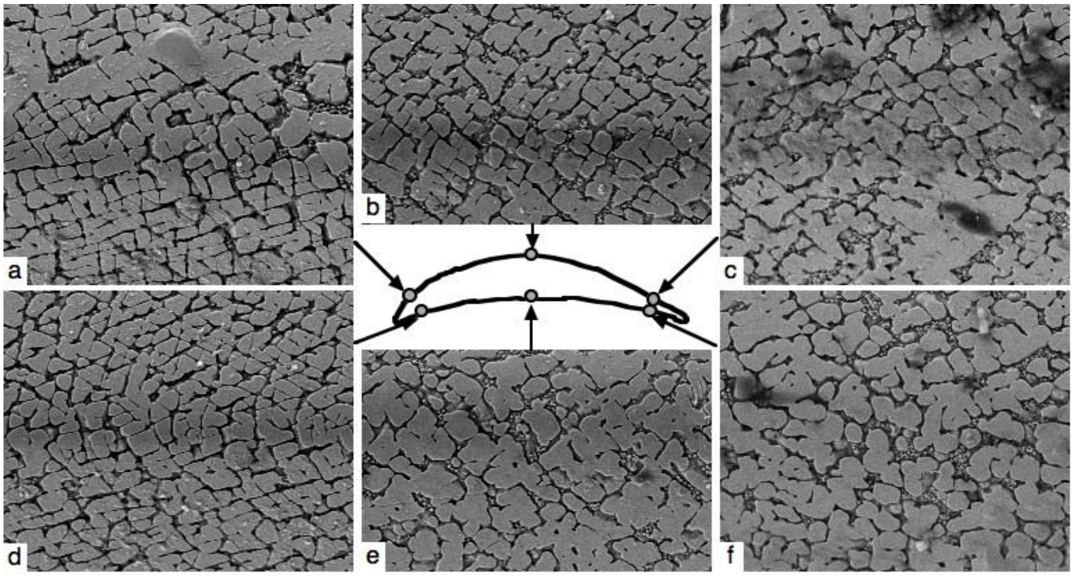

Figure 2. SEM micrographs of the suction and pressure sides of the 40mm part : the leading edge (a) and (d), 23mm portion (b) and (e) and the trailing edge (c) and (f), respectively.

3.2.3 70mm part

The SEM micrographs at the pressure and suction sides of the 70mm part are shown in Fig.3. Most of the γ' precipitates keep cuboidal in shape in all portions. There are few secondary γ' precipitates at the leading edge (Fig.3a,d), while the other portion, the secondary γ' precipitates are observed. The amount of the secondary γ' precipitates increased markedly toward the trailing edge. In particular, at the trailing edge, the secondary γ' precipitates are closely precipitated at the γ/γ' interfaces (Fig.3c,f).

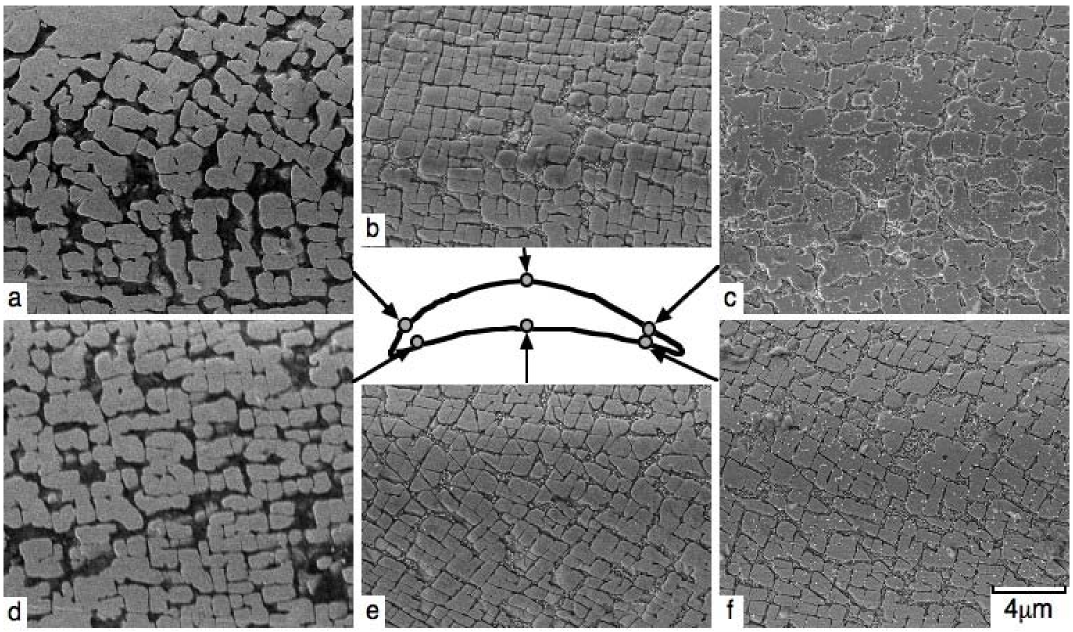

Figure 3. SEM micrographs of the suction and pressure sides of the 70mm part : the leading edge (a) and (d), 23mm portion (b) and (e) and the trailing edge (c) and (f), respectively.

3.2.4 Root part

The SEM micrographs at the pressure and suction sides of the root part are shown in Fig.4. Most of the γ' precipitates keep cuboidal in shape similar to the other part. At the suction side, a lot of the secondary γ' precipitates are observed in the γ matrix in the all portions, whereas the ratio of volume fraction of secondary γ' precipitates is high as leaving from the leading edge. At the 23mm portion and trailing edge, the fine secondary γ' precipitates in the γ matrix are closely precipitated at the γ/γ' interfaces (Fig.4b,c). At the pressure side, A large number of the fine secondary γ' precipitates are observed in all portions as well as the suction side (Fig.4d,f).

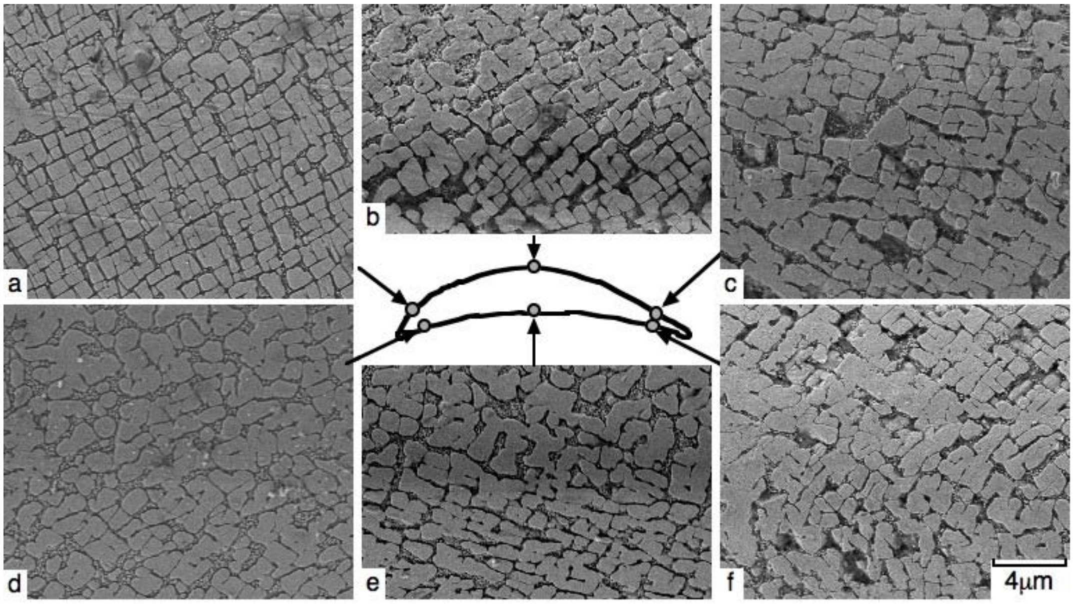

Figure 4. SEM micrographs of the suction and pressure sides of the root part : the leading edge (a) and (d), 23mm portion (b) and (e) and the trailing edge (c) and (f), respectively.

3.3 Estimation of the Temperature Distribution of Serviced Blade

The estimation of the temperature and the stress distribution of the blade in service is based on the morphology of γ' precipitates, that is, the formation of the rafted γ/γ' structures and the completion of them including the shape of the γ/γ' interfaces. However, as mentioned above, marked morphological changes from the cuboidal γ' precipitates to the rafted γ/γ' structures in each part of the blade are not observed in this work. Therefore, it is impossible to estimate the temperature and the stress distribution of the blade only based on the morphology of γ' precipitates. By the way, the secondary γ' precipitates in the γ matrix are dissolved and disappeared at high temperature, whereas with decreasing the temperature, the secondary γ' precipitates becomes smaller, and the denuded zone of ones near the γ' precipitates become narrow. Based on the above evidence, the temperature distribution of the blade in service will be estimated.

Fig.5 shows the schematic illustration of the temperature distribution of the blade in service. The temperature is classified into five from the morphology of the secondary γ' precipitates in the γ channel and the existence of one at the vicinity of the γ/γ' interfaces. The highest temperature is assumed that the secondary γ' precipitates had disappeared. The distribution from low temperature to high temperature is shown in shades from dark to light. At the suction side, the secondary γ' precipitates are not observed in the γ matrix at the leading and trailing edge of the tip part, temperature is relatively high. At the trailing edge side from the 40mm to the root parts where the many fine secondary γ' precipitates are precipitated in the γ matrix, the surface is exposed to the lowest temperature condition. At pressure side, at the leading edge side of the tip part and the leading edge of the 40mm part where the secondary γ' precipitates are disappeared, the surface is exposed to the highest temperature condition.

However, at the trailing edge side of the 70mm and root parts where the high amount of the fine secondary γ' precipitates exists at the vicinity of the γ/γ' interfaces in the γ matrix, the surface is not enough to be exposed to the high temperature condition.

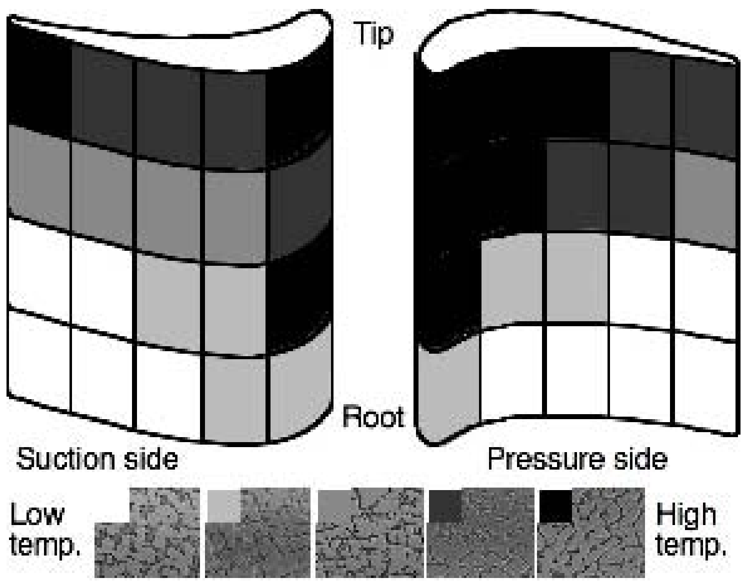

Figure 5. Schematic illustration of the distribution of the temperature of the 1st LPT blade in service.

3.4 Morphology of γ' Precipitates in Different Portion of Blade After Aging

As mentioned above, the cuboidal γ' precipitates of the as-heat treated single crystal Ni-based superalloy connected to three <100> directions and coarsened with simple aging at the high temperature. By employing the aging without stress of a single crystal Ni-based superalloy after the interrupted creep test at the stages when the γ' precipitates are still cuboidal, the γ/γ' structure changed to rafted one perpendicular to the creep interrupted stress axis.[15] Therefore, by subjecting the simple aging to the serviced blade, the morphological change of γ' precipitates, that is, the formation of the rafted γ/γ' structures is expected by the difference in the stress level. To estimate the distribution of the stress of the blade in service, the blade is aged at 1273K, 3.6×10^6s and the morphology of γ' precipitates is investigated on the aged specimens at the same portions before aging.

3.4.1 Tip part after aged

The SEM micrographs of the aged blade at the pressure and suction sides of the tip part are shown in Fig.6. There are no secondary γ' precipitates in γ matrix. At the suction side, coarsening of the γ' precipitates are observed (Fig.6a,c). At the pressure side, remarkable coarsening of the γ' precipitates are observed at the leading edge, whereas the degree of coarsening of the γ' precipitates is low as leaving from the trailing edge (Fig.6d,e).

ISSN 1516-392X

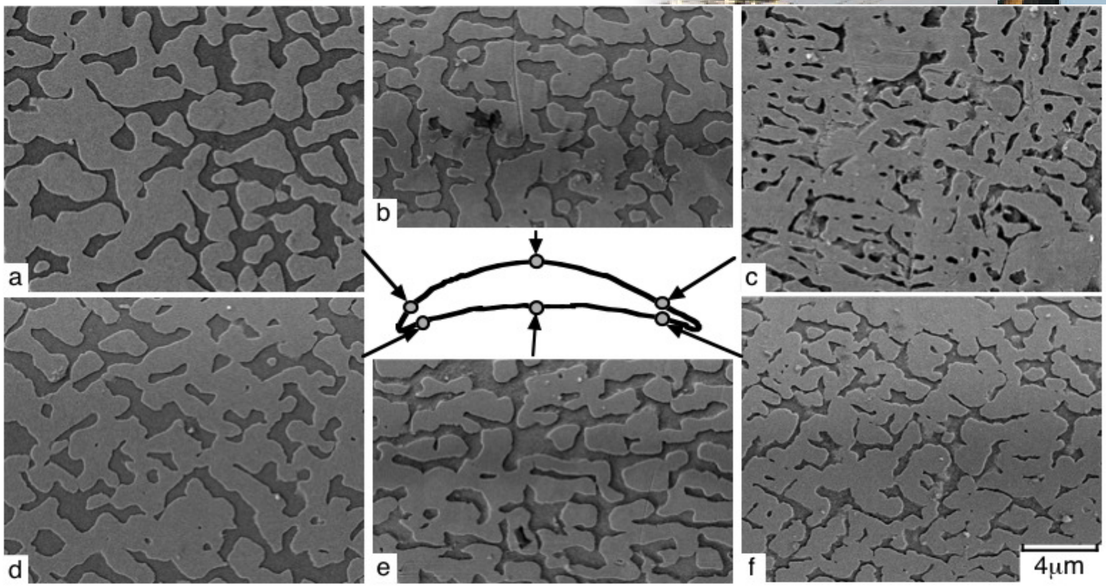

Figure 6. SEM micrographs of the aged blade of the suction and pressure sides of the tip part : the leading edge (a) and (d), 23mm portion (b) and (e) and the trailing edge (c) and (f), respectively.

3.4.2 40mm part after aged

The SEM micrographs of the aged blade at the pressure and suction sides of the 40mm part are shown in Fig.7. The adjacent γ' precipitates contact with each other. The secondary γ' precipitates are not observed in the γ matrix as well as the tip part.

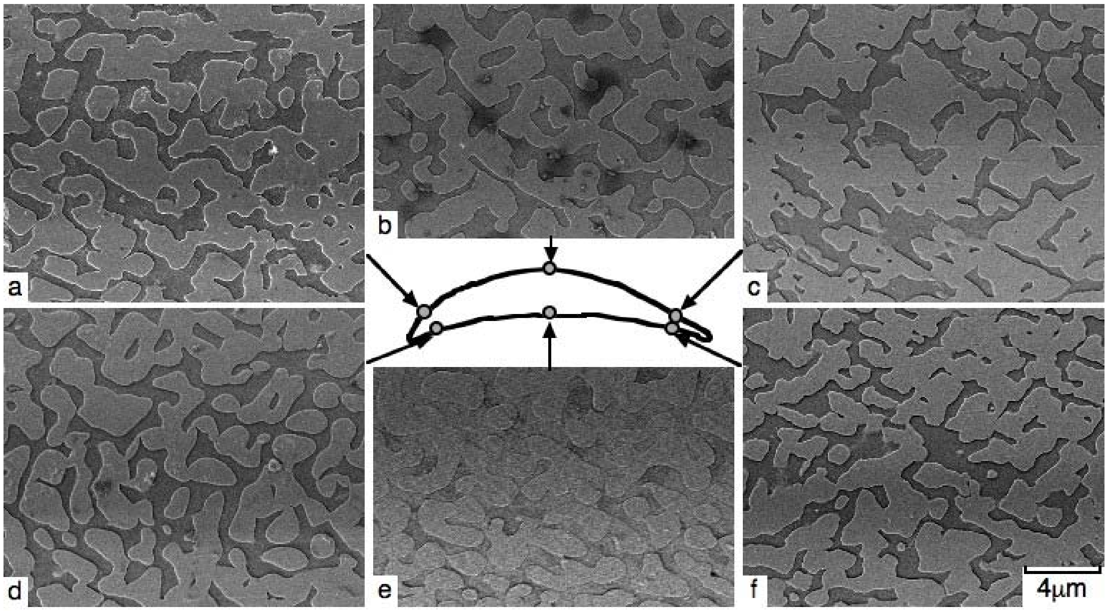

Figure 7. SEM micrographs of the aged blade of the suction and pressure sides of the 40mm part : the leading edge (a) and (d), 23mm portion (b) and (e) and the trailing edge (c) and (f), respectively.

3.4.3 70mm part after aged

The SEM micrographs of the aged blade at the pressure and suction sides of the 70mm part are shown in Fig.8. The secondary γ' precipitates are disappeared. At the suction side, most of the γ' precipitates are connected two specific directions, and the interface between the γ/γ' phase is straight (Fig.8a). At the 23mm portion, the rafted γ/γ' structure are observed, and the interface between the γ/γ' phase is also straight (Fig.8b). At the trailing edge, the low complete rafted γ/γ' structure are observed (Fig.8c).

At the pressure side, the morphology of the γ' precipitates are different from the suction side, further coarsening of the γ' precipitates are observed.

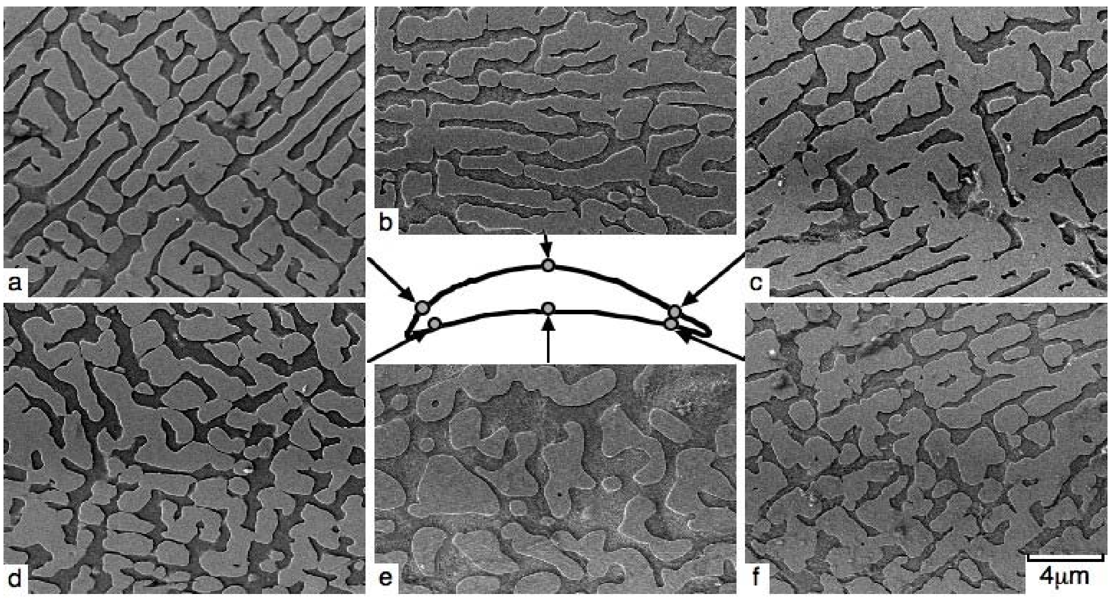

Figure 8. SEM micrographs of the aged blade of the suction and pressure sides of the 70mm part : the leading edge (a) and (d), 23mm portion (b) and (e) and the trailing edge (c) and (f), respectively.

3.4.4 Root part after aged

The SEM micrographs of the aged blade at the pressure and suction sides of the root part are shown in Fig.9. The rafted γ/γ' structures and the secondary γ' precipitates in the γ matrix are not observed in all portions.

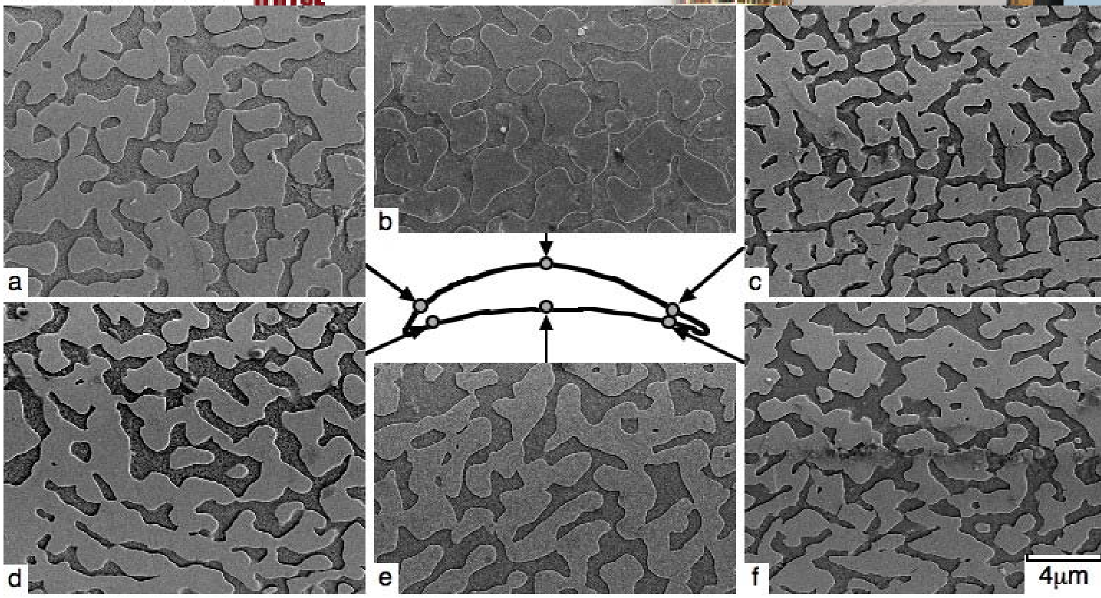

Figure 9. SEM micrographs of the aged blade of the suction and pressure sides of the root part : the leading edge (a) and (d), 23mm portion (b) and (e) and the trailing edge (c) and (f), respectively.

3.5 Estimation of the Stress Distribution of Serviced Blade

Based on the above microstructure evidences, the stress distribution of the blade in service will be discussed.

Fig.10 shows the schematic illustration of the stress distribution of the blade in service. The distribution from low temperature and low stress sides to high temperature and high stress sides is shown in shades from dark to light. The rafted γ/γ' structures are only appeared at the suction sides of 70mm part. However the completeness of the rafted γ/γ' structures is low. This microstructure evidence indicated that the amount of the deformation is extremely little, and the loaded stress is low on the 1st LPT blade in service. While most of the portions in the blade, coarsening of the γ' precipitates are observed. Therefore, it is supposed that there is almost no influence of stress.

Consequently, the stress for the 1st LPT blade in service is slightly high at the suction side of the 70mm part in comparison with other parts, but is extremely low overall.

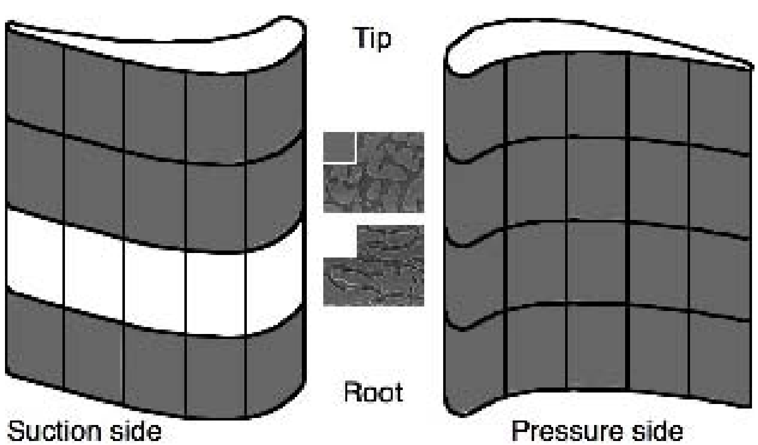

Figure 10. Schematic illustration of the distribution of the microstructure of the aged 1st LPT blade in service.

4 CONCLUSIONS

The morphology of the γ' precipitates of a Ni-based superalloy serviced as the 1st LPT blade of the jet engine and the one aged for 1273K, $3.6x10^6$s, are investigated to estimate the temperature and the stress distribution, and the stress directions in service. The following conclusions are obtained.

1) Most of the γ' precipitates kept cuboidal in shape in serviced blade.

2) The marked difference in the amount of the secondary γ' precipitates in each part of the blade are observed. There is no secondary γ' precipitates in the γ matrix at the pressure side and at the leading edge of suction side of the tip part, while at the root part, a large number of the fine secondary γ' precipitates are closely precipitated at the γ/γ' interfaces.

3) The surface at the leading edge side of the tip part and the leading edge of the 40mm part of the pressure side of the blade in service, are exposed to the highest temperature condition.

4) After simple aging, the low complete rafted γ/γ' structure are observed at the suction sides of 70mm part, while at the other portions, coarsening of the γ' precipitates is observed.

5) From these results on the 1st LPT blade in service, the temperature is exposed comparatively low, and the stress is slightly high at the suction side of the 70mm part in comparison with other parts, but is extremely low overall.

REFERENCES

1 H. Harada, "Superalloys, Present and Future," JSPS Rep. of the 123rd Committee on Heat Resisting Metals and Alloys, Vol.48, 2007, pp.357-365.

2 Y. Yoshioka, "Evolution of Superalloys as Gas Turbine Materials and Perspective on the Future," JSPS Rep. of the 123rd Committee on Heat Resisting Metals and Alloys, Vol.48, 2007, pp.367-377.

3 S. Walston, A. Cetel, R. MacKay, K. O'Hara D. Duhl and R. Dreshfield, "Joint Development of a Fourth Generation Single Crystal Superalloy," Proc. of 10th Int. Symp. on Superalloys2004, 2004, pp.15-24.

4 N. Miura, N. Harada, Y. Kondo and T. Matsuo, "Morphological Change in γ' Phase in Different Portions of First Stage High Pressure Turbine Blade of PWA1480," Proc. of the 7th Liege Conf. on Mater. for Adv. Power Eng. 2002, 2002, pp.245-254.

5 N. Miura, K. Nakata, M. Miyazaki, Y. Hayashi and Y. Kondo, "Morphology of γ' Precipitates in Second Stage High Pressure Turbine Blade of Single Crystal Ni-based Superalloy After Serviced," Materials Science Forum, Vols. 638-642, 2010, pp.2291-2296.

6 T. Fujimura, Mate. Tech. on Aircraft Gas Turbine Engines, J. of the Gas Turbine Soc. of Japan, Vol.32, 2004, p.174.

7 T. M. Pollock and A. S. Argon, "Creep resistance of CMSX-3 Nickel Base Superalloy Single Crystals," Acta Metall. Mater., Vol.40, 1992, pp.1-30.

8 M. Fahrmann, E. Fahrmann, O. Paris, P. Fratzl and T. M. Pollock, "An Experimental Study of the Role of Plasticity in the Rafting Kinetics of a Single Crystal Ni-base Superalloy," Proc. of the 8th Int. Symp. on Superalloys1996, 1996, pp.191-200.

9 D. Mukhherji, H. Gabrisch, W. Chen, H. J. Fecht and R. P. Wahi, "Mechanical Behavior and Microstructure Evolution in the Single Crystal Superalloy SC16," Acta Mater., Vol.44, 1997, pp.3143-3154.

10 N. Miura, Y. Kondo and T. Matsuo, "Stress Dependence of Strain Attained to Rafting of γ' phase in Single Crystal Ni-based Superalloy, CMSX-4," Proc. of 9th Int. Conf. on Creep and Fracture Eng. Mat. and Structures, 2001, pp. 437-445.

11 Y. Hayashi, N. Miura and Y. Kondo, Creep Resistance of Single Crystal Ni-based Superalloy, CMSX-4, at 1073K, CAMP-ISIJ, Vol.20, 2007, p.1229.

12 H. Biermann, B. V. Grossmann, T. Schneider, H. Feng and H. Mughrabi, "Investigation of the γ/γ' Morphology and Internal Stress in a Monocrystalline Turbine Blade After Service: Determination of the Local Thermal and Mechanical Loads," Proc. of the 8th Int. Symp. on Superalloys1996, 1996, pp.201-210.

13 M. Matsuoka, Aeronautics course 7, Jet Engine, Japan Aeronautical Engineers' Association, Tokyo, 2003, p.62.

14 Y. Hayashi, N. Miura, and Y. Kondo, "Microstructure in 1st Stage Low Pressure Turbine Blade of Polycrystalline Ni-based Superalloy After Serviced," Proc. of the 65th the Japan Society for Heat Treatment Meeting, 2007, pp.21-22.

15 N. Miura, K. Kurita, Y. Kondo and T. Matsuo, "Change in Morphology of γ' of Prior-crept Single Crystal Ni-based Superalloy, CMSX-4, With Simple Aging," Mat. Sci. Forum Vol. 539-543, 2007, pp.3024-3029.